Int. J. Electrochem. Sci., 6 **(2011)** 4953 - 4966

International Journal of
ELECTROCHEMICAL
SCIENCE
www.electrochemsci.org

A Magnetic-Controlled Amperometric Biosensor Based on Composite Bio-Particulates Fe_3O_4 and Nano-Au With The Signal Enhancement by Increasing Loading of Horseradish Peroxidase

Xiaoping Wei, Tao Liu, Jianping Li[*]*, Xuzhou Chen*

College of Chemistry and Bioengineering, Guilin University of Technology, Guilin, 541004, China
[*]E-mail: likianping@263.net

Received: 24 August 2011 / *Accepted:* 19 September 2011 / *Published:* 1 October 2011

A novel amperometric biosensor was developed to determine hydrogen peroxide (H_2O_2) by Fe_3O_4/Gold nanoparticles (nano-Au)/Horseradish peroxidase (HRP) bio-particulates modified electrode. Nano-Au was assembled onto the surface of mercapto-functional Fe_3O_4 nanoparticles via covalent linkages between nano-Au and cysteine thiol groups. HRP was adsorbed on the nano-Au to obtain Fe_3O_4/nano-Au/HRP bio-particles. The biosensor was fabricated by attaching the Fe_3O_4/nano-Au/HRP bio-particulates on the surface of a glassy carbon electrode by an external magnetic field. H_2O_2 was detected by using a hydroquinone mediator to transfer electrons between the electrode and HRP. The parameters of experimental variables of the enzymatic electrode were optimized and the effects of the condition on the analytical performance were discussed. The results showed that the biosensor had a fast response of less than 10 s in a linear range of 0 to 8.0×10^{-4} M, and the detection limit of H_2O_2 was 3×10^{-8} M at a signal-to-noise ratio of 3. The biosensor was easily fabricated and renewed with highly sensitivity due to increased surface area for HRP loading.

Keywords: Magnetic nanoparticles, Nano-Au, Biosensor, Horseradish peroxidase

1. INTRODUCTION

The immobilization of bioactive molecules on the surface of magnetic nanoparticles has received great interest in recent years [1, 2]. Modified with functional macromolecules, such as enzymes, antibodies, DNA or RNA, these bioconjugates are widely used in drug targeting, controlled drug release, enzyme immobilization, immunoassay, separation of DNA or cells, and development of highly activated catalysts [3, 4]. Due to their biocompatible activity and low toxicity, utilizing magnetic nanoparticles has held great potential for biosensors applications [5-7]. The immobilization

of enzymes on magnetic nanoparticles has been reported with potential advantage in bioactive particles with their unique characters, such as enhancing enzymatic activity and rapid contacting between the enzyme and its substrate, and reduce mass-transfer limitations. Ultimately, the immobilization of enzymes on magnetic nanoparticles result in a reduction of mass-transfer limitations between the enzyme and the analyte due to the good dispersion of the analyte in the solution [8, 9]. On the other hand, magnetic nanoparticles, for example, Fe_3O_4 nanoparticles are high chemical activity and easily oxidized in air. It is very difficult to immobilize enzyme onto the surface of the particle. Grafting or coating the nanoparticle with organic species (e.g., surfactants or polymers) or inorganic layers (e.g., silica or carbon) have been attempted, but the ultimate average size of the particle was increased and the enzyme activity was decreased. For which, its application as electrochemical biosensors was restricted. Thus, developing methodologies for the modification of the surface properties of magnetic nanoparticles using new nano-materials is still necessary.

Gold nanoparticles (nano-Au) have a very large surface, which could be used to immobilize enzymes with well-retained bioactivity and biocompatibility [10]. The use of nano-Au for the preparation of biosensors has been attracting increasing interests due to it's signal amplification [11]. Recently, many reports have demonstrated that nano-Au can adsorb redox enzymes without a loss of biological activity. They have also been found to facilitate electron transfer between an electrode and enzyme in a biosensor. Consequently, with increased adsorption and activity, the sensitivity of the sensors [12-15] could be enhanced.

Hydrogen peroxide (H_2O_2) results from reactions that are catalyzed by many types of oxidases. The determination of H_2O_2 is very important and has great practical value in various applications, such as chemistry, biology, clinical studies, and so on. The properties of renewable H_2O_2 biosensors could be improved by immobilizing horseradish peroxidase (HRP) on magnetic nanoparticles via embedding, covalent bonding and adsorption in order to form magnetic bio-particles, which could be controlled by a magnetic field [16-24]. However, the sensitivities of the biosensors need to be heightened by increasing the loading amount of the enzyme and their bioactivity.

In this work, nano-Au was assembled onto magnetic nanoparticles and used to immobilize HRP to form nano-Au modified magnetic bio-particle by electrostatic adsorption and physical adsorption. Using magnetic force, a novel H_2O_2 biosensor was fabricated by attaching the magnetic bio-particles. The sensor is highly sensitive due to the increasing surface area for HRP loading. Also, it is convenient and easily renewable.

2. EXPERIMENTAL

2.1. Reagent and materials

$FeCl_3 \cdot 6H_2O$ and $FeCl_2 \cdot 4H_2O$ were obtained from Guangdong, China. $AuCl_3 \cdot HCl \cdot 4H_2O$ (wt(Au)≥ 47.8%) was obtained from Aldrich. *L*-cysteine was obtained from Shanghai, China. HRP (E.C.1.11.1.7, Rz > 3.0, 250 U/mg) was purchased from Sigma and used as received. A 30% hydrogen peroxide solution was purchased from Beijing Chemical Reagent (Beijing, China), and a fresh solution

of H_2O_2 was prepared daily. The 0.067 M phosphate buffer solutions were used as supporting electrolytes by mixing solution Na_2HPO_4 and KH_2PO_4 [25]. Unless otherwise stated, all chemicals and reagents used were of analytical grade. All solutions were prepared using double distilled water.

2.2. Apparatus

Cyclic voltammetric and amperometric experiments were performed with a CHI 660B electrochemical workstation (Shanghai Chenhua Instrument Co, China). A conventional three-electrode system was employed, consisting of a glassy carbon disk electrode (3 mm diameter) modified with Fe_3O_4/Au/HRP modified serving as a working electrode, while saturated calomel electrode (SCE) and platinum wire served as the reference and counter electrode, respectively. All potentials are referenced to the SCE. Cyclic voltammetric measurements and amperometric experiments were carried out in a thermostat (25 $^{\circ}$C). A nitrogen environment was then kept over solutions in the cell. A magnet and an iron bar were used to fabricate the biosensor.

2.3. Preparation of colloidal gold

The colloidal gold sol was prepared according to the method developed by Frens [26]. All glasswares used in this preparation were thoroughly cleaned in a bath of freshly prepared HNO_3/HCl (3/1) solution and rinsed in double distilled water. Aqueous solutions of $HAuCl_4$ and trisodium citrate were filtered through a 22 μm microporous membrane filter prior to use. In a 250 mL round-bottom flask, 100 mL of 0.1 wt% $HAuCl_4$ solution was brought to a boil with vigorous stirring. Then, 2.5 mL of 2 wt% trisodium citrate was rapidly added into this solution, resulting in color change from blue to red-violet. The mixture was continually boiled for an additional 10 min and stirred for another 10 min upon removal of the heater. The obtained colloidal gold solution was then cooled to room temperature and stored in dark bottles at 4 $^{\circ}$C.

2.4. Preparation of nanosized Fe_3O_4 particles and thiol functionalization

In this work, magnetite nanoparticles (Fe_3O_4) were prepared according to a previously reported procedure [25]. In order to produce particles with a narrow size distribution, a magnetite ferrofluid was prepared from $FeCl_3$ and $FeCl_2$ in water at a temperature of 35 $^{\circ}$C maintained by a thermostat water bath. The ratio between Fe^{3+}/Fe^{2+} was 2:1.2. For the precipitation, a solution of 1 M NaOH solution was carefully added to the solution with vigorous stirring at 50 $^{\circ}$C. The pH value was adjusted to 10 by adding the necessary amount of 1 M NaOH to the aqueous solution. The temperature of water bath was adjusted to 80 $^{\circ}$C, and the solution was stirred for another 1 h. The whole reaction process was protected with highly pure nitrogen. The black mixture was centrifuged and washed with double distilled water for three times before vacuum-drying in furnace at 60 $^{\circ}$C for 6 h.

Prior to construct the biosensor, *L*-cysteine was loaded onto Fe_3O_4 nanoparticles via condensation reaction [25, 27]. Iron oxide nanoparticles (50 mg) were re-dispersed in 50 mL double

distilled water by sonication. Then, 5 mL *L*-cysteine solution (1 mg/mL) was mixed with the solution by mechanical stirring. The pH value of the aqueous solution was adjusted to 5.8 by adding 0.1 M HCl or 0.1 M NaOH solution. The solution was continuously stirred overnight under nitrogen at room temperature. The obtained black precipitate was separated by magnetic decantation and washed with double distilled water for three times. The resulting *L*-cysteine-modified magnetic nanoparticle was obtained.

2.5. Synthesis of Fe_3O_4/nano-Au/HRP bio-particles

Under nitrogen protection, 10 mL Fe_3O_4/Cys magnetic nanoparticles (2.0 mg/mL) were re-dispersed by sonication. A 2 mL portion of colloidal gold was added with constant stirring overnight. The nanoparticles were separated by magnetic decantation, washed, and re-suspended in a 10 mL buffer solution. The resulting nano-Au modified magnetic particle was recorded as Fe_3O_4/nano-Au. An HRP solution was prepared by dissolving 10 mg enzyme in 5 mL phosphate buffer solution (PBS) at pH 7.0. The Fe_3O_4/nano-Au suspension was combined with 2 mL enzyme solution with mechanical stirring overnight at 4 °C. The excess HRP was removed by washing with PBS (pH 7.0) three times. The obtained Fe_3O_4/nano-Au/HRP magnetic bio-particles were stored at 4 °C until use. The process of fabricating the magnetic bio-particles is briefly described in Scheme 1.

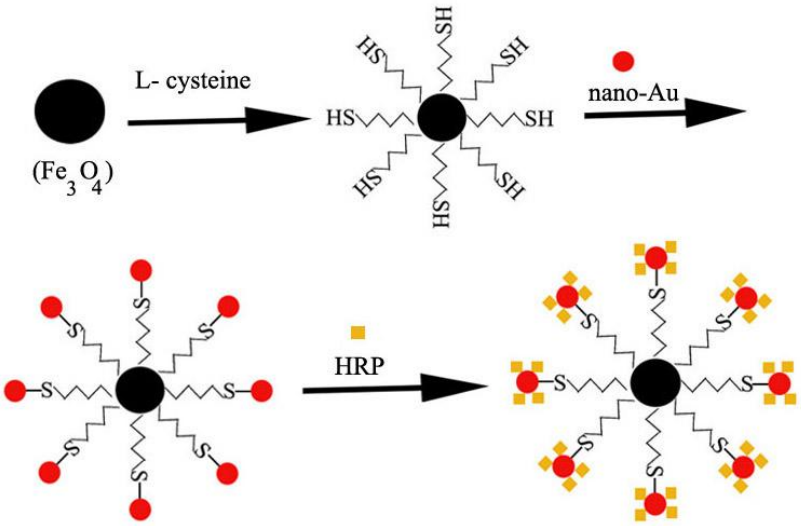

Scheme 1. A schematic showing the steps involved in the fabrication of Fe_3O_4/Nano-Au/HRP magnetic bio-particles

2.6. Preparation of the iron core-glassy carbon electrode

A glassy carbon electrode with an iron core was fabricated by filling melted solid paraffin carbon paste into a glass tube 3 cm in length, after which an iron bar was inserted from the other end. The ion bar was chosen to act as the magnetic conductor and the electro-conductor of the electrode. A

glassy carbon wafer (2 mm in diameter) was cut and immobilized on the end of the solid paraffin carbon paste electrode with epoxy resin mixed with carbon powder. The glassy carbon was then consecutively polished with 1.0, 0.3, and 0.05 μm alumina slurry, followed by rinsing thoroughly with double distilled water after each step. Then, the electrodes were successively sonicated in 1:1 nitric acid, ethanol, and distilled water.

2.7. Preparation of the biosensor

The Fe_3O_4/nano-Au/HRP magnetic bio-particles were suspended in 1 mL PBS (pH 7.0). Then, 10 μL suspension was dropped onto the inverted electrode, dried for 15 min. The electrode surface was washed with PBS to remove the excess bio-particles. With the help of a permanent magnet, which was placed at the end of the iron bar, the magnetic bio-particles were firmly attached to the electrode surface, completing the fabrication of the enzyme electrode. The biosensor was stored in a moist state at 4 $^{\circ}$C when not in use.

3. RESULTS AND DISCUSSION

3.1. Particle size analysis, x-ray energy-dispersive spectroscopy, and magnetic measurement of Fe_3O_4/nano-Au particles

Nano-Au particle size distributions were measured with a laser particle size analyzer (Malvern Zetasizer Nano-90). The diameter of the Au nanoparticles is narrowly distributed at 20 nm. The diameters of the Fe_3O_4 nanoparticles were ranged from 20-25 nm.

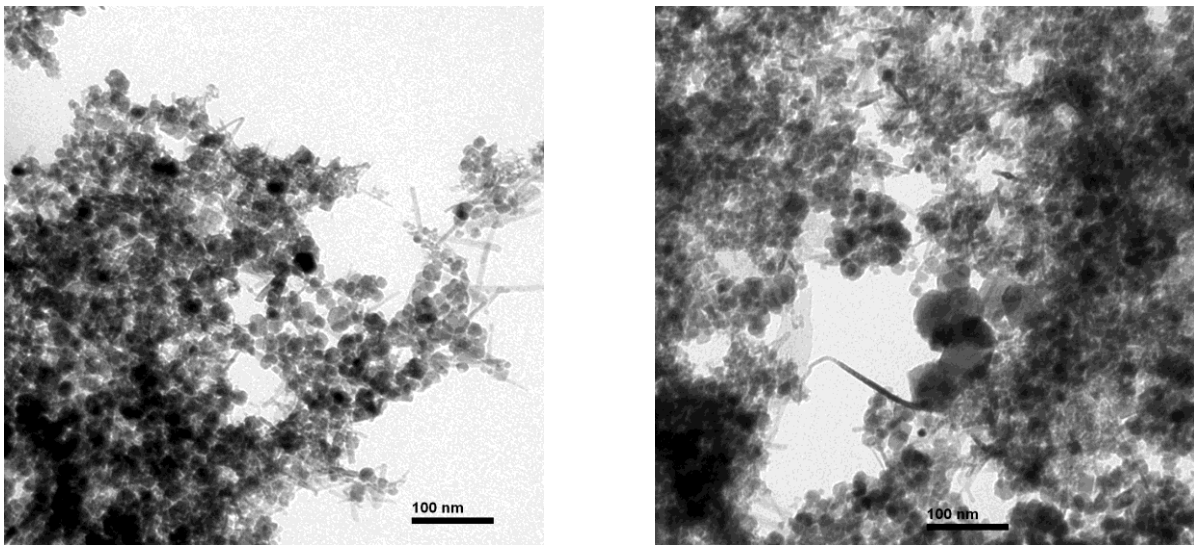

Figure 1. Transmission electron microscopy images of Fe_3O_4/Nano-Au (a) and Fe_3O_4/Nano-Au/HRP (b)

The transmission electron microscopy (TEM) image was obtained using a JEOL model JEM 2000EX (Japan) instrument, operating at voltage of 120 kV. Figure 1 shows the TEM images of Fe_3O_4/Nano-Au (a) and Fe_3O_4/Nano-Au/HRP (b). It is seen that the Au/Fe_3O_4 nanoparticles were composited with Au and Fe_3O_4 nanoparticles. The average diameter of the Fe_3O_4/Nano-Au/HRP composite nanoparticles increased slightly comparing with Fe_3O_4/Nano-Au, with no presence of integration.

In order to characterize the composition of the Fe_3O_4/nano-Au, some samples were dried in a vacuum furnace at 60 °C for 12 h and then analyzed by energy dispersive x-ray spectroscopy (EDS). Based on the EDS spectra (Fig. 2), the dominant elements in the magnetic particles were Fe, O, and Au, and the mass percentage of each are 29.75% (Fe), 35.06% (O), and 19.36% (Au), respectively. The result demonstrated that nano-Au particles have been assembled successfully on the surface of Fe_3O_4.

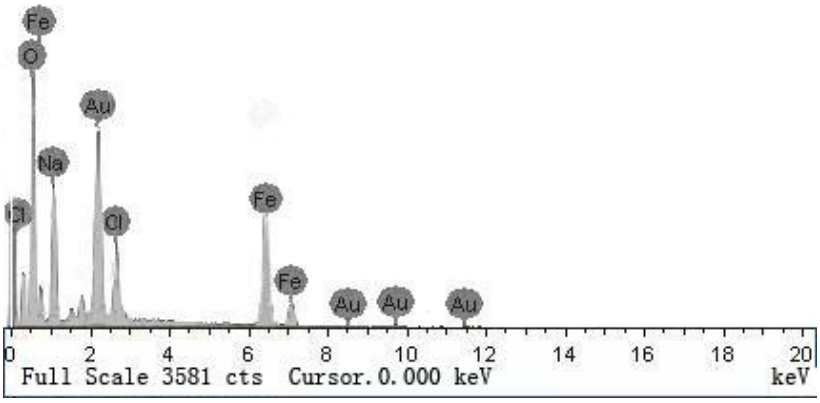

Figure 2. EDS spectrum of the Fe_3O_4/nano-Au particles

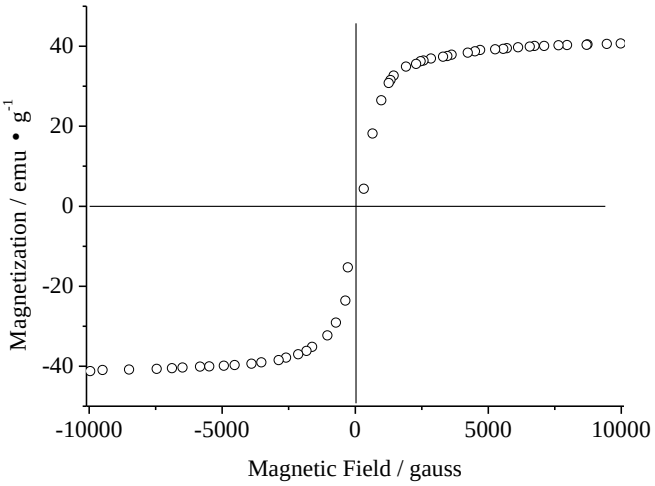

Figure 3. Hysteresis curves of the Fe_3O_4/nano-Au magnetic particles

The magnetic hysteresis loop of Fe_3O_4/nano-Au magnetic particles is shown in Fig. 3. The specific saturation magnetization reached 40.09 emu/g, indicating that the nanoparticles exhibited ideal magnetic properties. No remanence is detected, indicating an ultra-paramagnetic property, which is useful for separating magnetic particles from the solution using an external magnetic field.

3.2. Fabrication mechanism of Fe_3O_4/nano-Au/HRP magnetic bio-particles

In this work, the Fe_3O_4 nanoparticles were prepared using a chemical co-precipitation technique in an aqueous solution. Many hydroxyl groups exist around the metal oxide in an aqueous solution, and the isoelectric point of the Fe_3O_4 solution was obtained at 6.53 by Chang et al. [28]. The Fe_3O_4 particles are negatively charged in an aqueous solution when the pH value is over 6.53, while these are positively charged when the pH value is below 6.53. Cysteine strongly adsorbs on the Fe_3O_4 nanoparticles mainly because of electrostatic interactions, hydrogen bonding, and other types of chemical bonding. Furthermore, the adsorption process is irreversible, so the cysteine adsorbed on Fe_3O_4 nanoparticles are difficult to desorb. Thus, the pH value of the Fe_3O_4 suspension is adjusted to 5.8 for this experiment. Nano-Au is assembled easily on the mercapto-functionalized Fe_3O_4 particle through cysteine, specifically due to the Au–S bond. The nano-Au carries negative charges because it was prepared through a citrate reduction of $HAuCl_4$. The citrate ions with negative charges serve as a stabilizing agent for the colloidal Au. The isoelectric point of HRP is 7.4 [29], so the HRP molecules are positively charged at pH 7.0. Therefore, HRP can be strongly adsorbed on magnetic nano-Au particles due to electrostatic interactions.

3.3. Electrocatalytic behavior of the biosensor for the reduction of H_2O_2

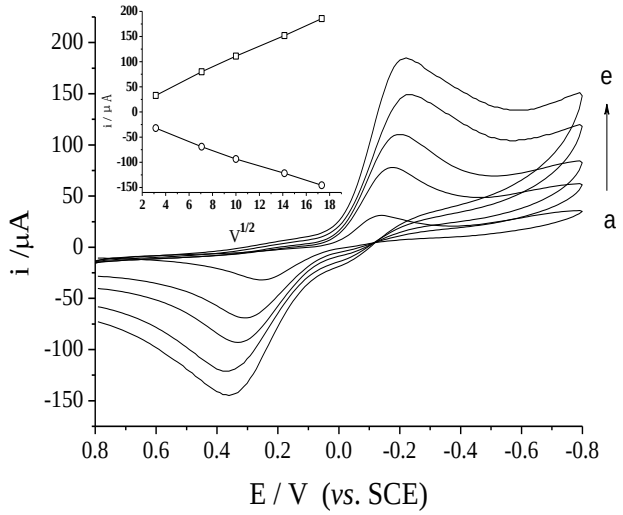

Figure 4. Cyclic voltammograms recorded at scan rates of 10, 50, 100, 200, and 300 mV/s (a-e) in 0.067 M PBS (pH 7.0) containing 1.0 mM hydroquinone

Figure 3 displays the cyclic voltammograms recorded for the enzymatic electrode in 0.067 M PBS (pH 7.0) containing 1×10^{-3} M hydroquinone at different scan rates. Both the redox peak currents increase with an increase in scan rate. The reduction and oxidation peak currents (i_{pa} and i_{pc}) are proportional to the square root of the scan rate ($v^{1/2}$) (inset in Fig. 4). Thus, the electrode reaction is typical of a diffusion-controlled process.

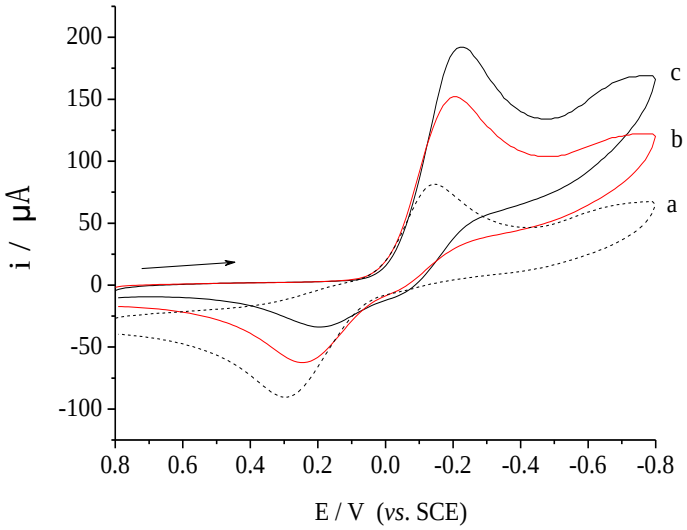

Figure 5. Cyclic voltammograms recorded in 1.0 mM hydroquinone solution in the absence of H_2O_2 (a) and in the presence of 0.2 mM H_2O_2 (b) and 0.5 mM H_2O_2 (c) for the Fe_3O_4/nano-Au/HRP-modified electrode. Supporting electrolyte: PBS (pH 7.0). Scan rate: 50 mV/s

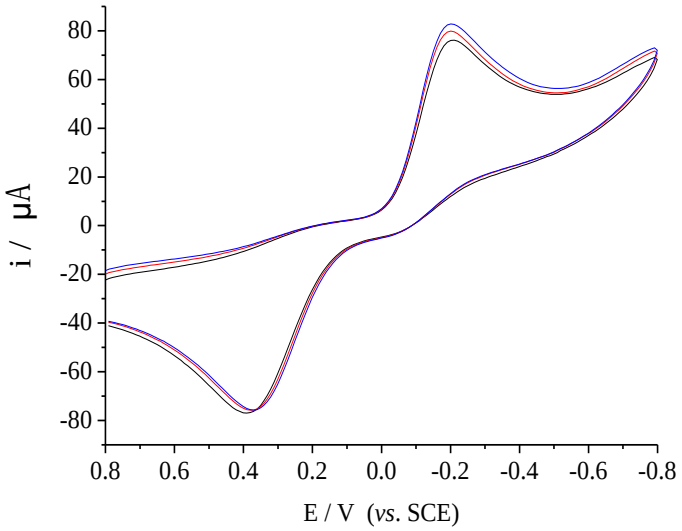

Figure 6. Cyclic voltammograms recorded in 1.0 mM hydroquinone solution in the absence of H_2O_2 (a) and in the presence of 0.2 mM H_2O_2 (b) and 0.5 mM H_2O_2 (c) for the Fe_3O_4/nano-Au-modified electrode. Supporting electrolyte: PBS (pH 7.0). Scan rate: 50 mV/s

The electrocatalytic behavior of the enzyme electrode for the electrochemical reduction of H_2O_2 is studied using cyclic voltammetric method. Figure 5 shows the cyclic voltammograms of the Fe_3O_4/nano-Au/HRP-modified electrode in unstirred deoxygenated 0.067 M PBS (pH 7.0) containing 1×10^{-3} M hydroquinone at a scan rate of 50 mV/s. In the absence of H_2O_2 (Fig. 5a), only a single pair of reversible oxidation/reduction peak is observed. This represented the typical electrochemical behavior of hydroquinone. However, in the presence of 0.2 mM H_2O_2 (Fig. 5b), an obvious increase of the reduction current and a concomitant decrease of the oxidation current is observed. The oxidation current further decreases, while the reduction current increases when 0.5 mM H_2O_2 is added (Fig. 5c). To verify whether significant electrocatalytic behavior is mainly due to the presence of H_2O_2, a control experiment is done in the absence of HRP. Figure 6 shows the cyclic voltammograms of Fe_3O_4/nano-Au-modified electrodes recorded at the same condition stated above. No obvious change is observed. The results showed that HRP has been immobilized successfully on the magnetic particles. The Fe_3O_4/nano-Au/HRP magnetic bio-particles immobilized on the electrode possess improved electrocatalytic ability for H_2O_2 reduction. Moreover, hydroquinone can effectively shuttle electrons from the redox center of the HRP molecules immobilized on the magnetic particles to the glassy carbon electrode. The electrocatalytic process can be expressed as follows [30]:

$$\text{HRP} + H_2O_2 \rightarrow \text{HRP-I} + H_2O \quad (1)$$

$$\text{HRP-I} + M_0 \rightarrow \text{HRP-II} + M_1 \quad (2)$$

$$\text{HRP-II} + M_0 \rightarrow \text{HRP} + M_1 \quad (3)$$

$$M_1 + 2e \rightarrow M_0 \quad (4)$$

$$\text{Net reaction: } H_2O_2 + 2e + 2H^+ \rightarrow 2H_2O \quad (5)$$

where HRP, HRP-I and HRP-II represent the enzyme peroxidase in the native form and in its two oxidized forms, respectively; M_0 is hydroquinone; and M_1 is benzoquinone, the oxidation product of M_0.

3.4. Optimization of measurement variables

The effect of hydroquinone concentration on the biosensor response was investigated in PBS (pH 7.0) in the presence of 0.5 mM H_2O_2 using chronoamperometry with an applied potential of -0.18 V. The responsive currents of the Fe_3O_4/nano-Au/HRP-modified electrode increase sharply with an increase in hydroquinone concentrations from 5.0×10^{-5} M to 1.0×10^{-3} M, before leveling off. This is a typical characteristic of a mediator-based sensor. The current response is mainly limited by enzyme-medium kinetics when the medium is low in the concentration, whereas it is limited by enzyme-substrate kinetics when the medium is high in the concentration. However, a higher hydroquinone

concentration causes a higher background current. Therefore, a hydroquinone concentration of 1.0 m M was selected for further experiments.

The effects of the pH value on the response currents of the biosensor were studied between 5.0 and 8.0 in 0.067 M PBS in the presence of 0.5 mM H_2O_2 using chronoamperometry with an applied potential of -0.18 V. The current response increases from pH 5.0 to 7.0, and a maximum value is achieved at pH 7.0, before decreasing from pH 7.0 to 8.0 (Fig. 7, curve a). This result is in agreement with that reported for soluble HRP [31, 32] and shows that the assembled Au nanoparticles have not altered the optimal pH value for the bioelectrocatalytic reaction of the immobilized HRP for H_2O_2. In order to obtain maximum sensitivity and bioactivity, a pH level of 7.0 was adopted in the following tests.

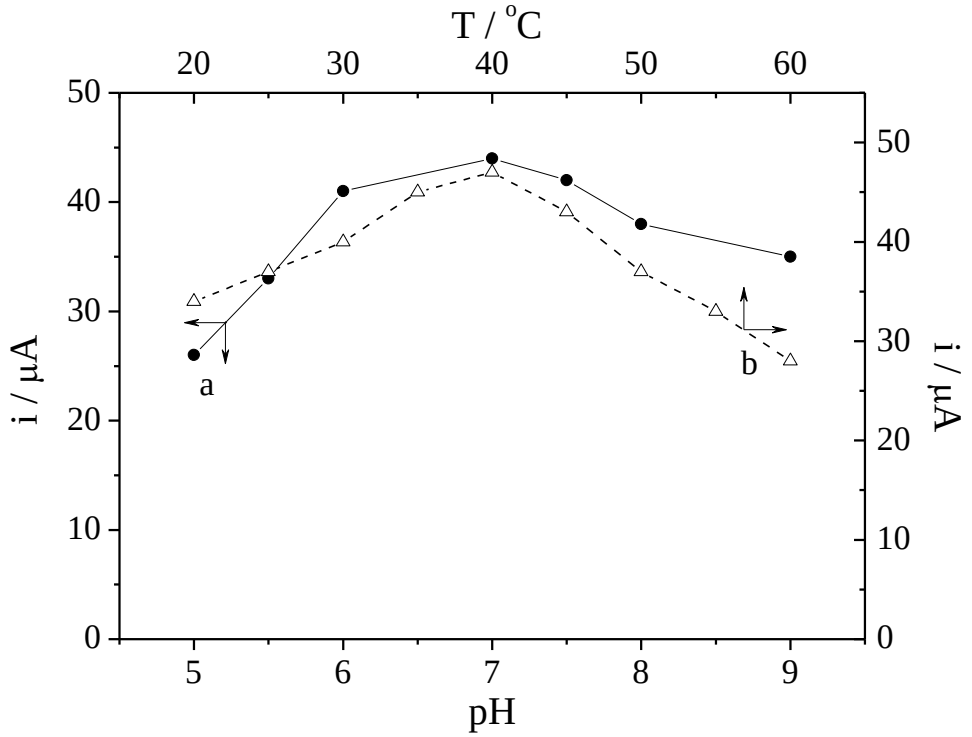

Figure 7. Effects of pH of the PBS solution (a) and temperature (b) on current responses of the biosensor to 0.5 mM H_2O_2 in PBS containing 1.0 mM hydroquinone at an applied potential of -0.18 V (*vs.* SCE)

The influence of the supporting electrolyte temperature on the steady-state currents of the biosensor was tested from 15 to 60 °C. The response currents gradually increase from 15 °C to 40 °C, before decreasing as the temperature reached over 40 °C. This behavior can be mainly attributed to the thermal inactivation of immobilized HRP on the biosensor (Fig. 7, curve b). The response current reaches a maximum at 40 °C, and a higher temperature leads to a shorter biosensor lifespan. Therefore, the temperature is set at 30 °C for the following experiments.

Figure 8 shows the applied potential dependence of the steady-state currents of the biosensor over a potential range of 0 to -0.25 V with 0.5 mM H_2O_2 in PBS (pH 7.0) containing 1.0 mM

hydroquinone. The steady-state current increases steadily when the applied potential shifts negatively from 0 to -0.18 V, since the enzymatically liberated benzoquinone species can be reduced easily at a more negative potential. However, when the potential is further stepped negatively, the response currents actually level off. In this work, -0.18 V was chosen as the applied potential for the amperometric determination of H_2O_2, so that the risk of interfering with the reactions of other electroactive species in the solution can be minimized. Furthermore, the background current and noise levels reach their lowest values at this potential.

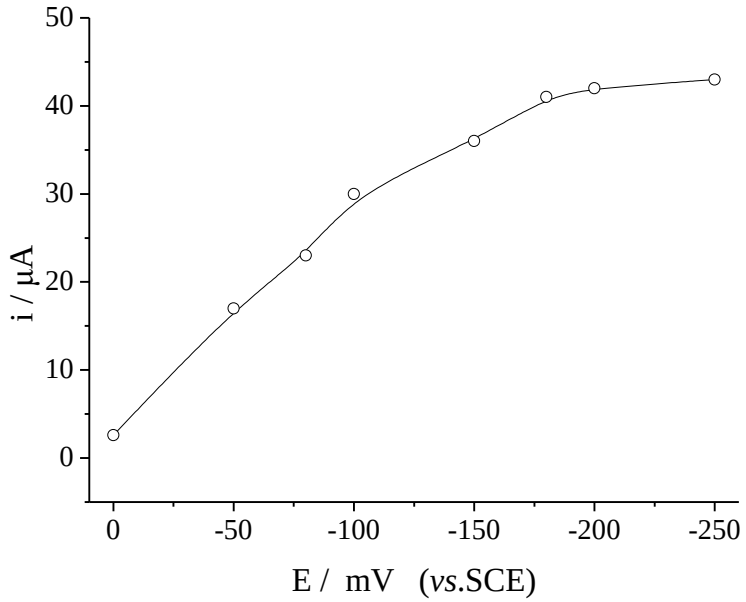

Figure 8. Effects of the applied potential on the current response of the biosensor to 0.5 mM H_2O_2 in PBS (pH 7.0) containing 1.0 mM hydroquinone

3.5. Chronoamperometric response and calibration curve

Figure 9 shows a typical current–time plot for the biosensor obtained upon adding different aliquots of H_2O_2 to PBS (pH 7.0) while stirring and at an applied potential of -0.18 V. With an increase of substrate concentration, the biosensor responds rapidly and a 95% steady-state current is reached within 10 s, indicating an excellent electrocatalytic behavior from the nanoparticle-based enzyme biosensor.

The calibration curve of the response current and the concentration of H_2O_2 are shown in the inset image of Fig. 9. As can be seen, a linear response curve is observed for H_2O_2 detection from 0 to 8.0×10^{-4} M H_2O_2 with a correlation coefficient of 0.9993 (n=9). The detection limit is found to be 3×10^{-8} M at a signal-to-noise ratio of 3. The detect limit of the sensor is lower than the traditional HRP modified gold electrodes reported [33-35], it is probably owing to the large loading capacity of HRP on magnetic nanoparticles.

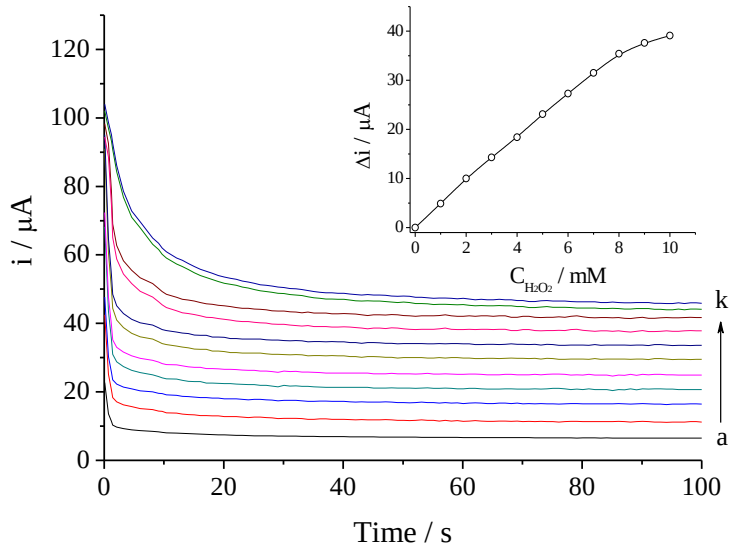

Figure 9. Chronoamperometric response of the biosensor after additions of 0 (a), 0.1 (b), 0.2 (c), 0.3 (d), 0.4 (e), 0.5 (f), 0.6 (g), 0.7 (h), 0.8 (i), 0.9 and (j), 1.0 mM H_2O_2 (k) into 0.067 M PBS (pH 7.0) containing 1.0 mM hydroquinone at an applied potential of -0.18 V (*vs*. SCE)

3.6. Reproducibility, stability, and selectivity

The repeatability of the current response of the biosensor to 5×10^{-5} M H_2O_2 was examined. The relative standard deviation (RSD) is 2.6% for eight successive assays. The electrode-to-electrode reproducibility examined from the response to 0.5×10^{-5} M H_2O_2 between five different electrodes that were made independently following the same scheme shows an acceptable reproducibility with an RSD of 4.5%. Good reproducibility may be due to the fact that HRP molecules are attached firmly onto the surface of nano-Au and that the amount of Fe_3O_4/nano-Au/HRP particles is consistent. Comparing with traditional modified electrode, the electrode was easy to generate and showed an excellent repeatability.

The magnetic bio-particles for biosensor preparation were stored in a moist state at 4 °C when not in use. The stability of the biosensor was investigated by measuring the current response with 5.0×10^{-5} M H_2O_2 every three days.

After four weeks, the response current is maintained at a value of 92% of the initial response, and, after eight weeks, the value decreases slightly to 80%. The loss of the current response of the biosensor may be attributed to a decrease of HRP activity during storage. Thus, the magnetic-controlled nanoparticle-enzyme electrode is quite efficient in retaining HRP activity. Good storage stability can be attributed to the fact that colloidal Au nanoparticles have good biocompatibility and suitability for protein immobilization.

The effects of substances that might interfere with the response of the proposed biosensor were also studied. The potential interfering substances, including glucose, sucrose, ethanol, acetic acid, citric acid, acetaminophenol, oxalic acid and ascorbic acid, were examined. Afterwards, interference experiments were performed in PBS at optimal conditions by comparing the response current of

5.0×10^{-5} M H_2O_2 plus 1.0 mM of each interfering substance with experiments using pure 5.0×10^{-5} M H_2O_2. The results show that 1×10^{-4} M ascorbic acid interferes significantly in the determination of H_2O_2. This may be attributed to H_2O_2 consumption involving the oxidation of ascorbic acid. Other substances do not cause any observable interference at a concentration of 1×10^{-3} M.

3.7. Apparent Michaelis-Menten constant

The apparent Michaelis-Menten constant (K_m) can be calculated from the electrochemical version of the Lineweaver-Burk equation:

$$1/i_{ss} = (K_m / i_{max}) \times (1/C) + 1/i_{max} \quad (6)$$

where i_{ss} is the steady-state current after the addition of substrate, C is the bulk concentration of the substrate, and i_{max} is the maximum current measured under saturated substrate conditions. The value of K_m for the biosensor is determined to be at 0.31 mM by the steady-state amperometric response.

This value is smaller than that of the native system in a buffer solution. The decrease may result from the bioactivity and biocompatibility of nano-Au. The method for the immobilization of the enzyme appears to be beneficial for improving the biosensor performance.

3.8. Analysis of samples

A commercial H_2O_2 disinfector from Lin'an Chemical Co. was analyzed using the proposed method (biosensor) described above. Before the experiment, the samples were diluted 10 times with PBS. A potassium permanganate titration method for H_2O_2 acted as a reference method to verify the accuracy. The results show that the relative standard deviations are 0.8-3.2% and that the deviations between both methods are within the range of ± 3.9%.

4. CONCLUSIONS

The assembling-type Fe_3O_4/nano-Au/HRP magnetic bio-particles were synthesized and shown to have acceptable ultra-paramagnetism. The HRP enzymes were proven to be immobilized on the nano-Au-modified magnetic nanoparticle without a loss of biological activity. The novel H_2O_2 biosensor based on magnetic bio-particles immobilized by magnetic forces exhibited fast amperometric response, low detection limit, and broad linear range for H_2O_2 detection. Moreover, the proposed biosensor was easy to fabricate and can be renewed conveniently due to the magnetic-controlled technique. The approach presented in this paper provides a simple method for developing a renewable amperometric biosensor.

ACKNOWLEDGMENTS
The authors gratefully acknowledge the financial support from the National Science Foundation of China (No. 21165007) and the Natural Science Foundation of Guangxi Province (No. 0728214).

References

1. B.I. Haukanes and C. Kvam, *Nat. Biotechnol*., 11 (1993) 60-63
2. A.H. Lu, E. L. Salabas and F. Schüth, *Angew. Chem. Int. Ed.*, 46 (2007) 1222-1244
3. T. Goetze, C. Gansau, N. Buske, M. Roeder, P. Görnert and M. Bahr, *J. Magn. Magn. Mater*, 252 (2002) 399-402
4. V. Polshettiwar, R. Luque, A. Fihri, H. Zhu, M. Bouhrara and J.-M. Basset. *Chem. Rev.*, 111 (2011) 3036–3075
5. E. Katz, I. Willner and J. Wang, *Electroanalysis*, 16 (2004) 19-44
6. Z.G. Xiong, J.P. Li, L. Tang and Z.Q. Chen, *Chinese J. Anal. Chem.*, 38 (2010) 800-804
7. H. Yin, Y. Zhou, T. Liu, T. Tang, S. Ai and L. Zhu. *J. Solid State Electrochem*., (2011) DOI: 10.1007/s10008-011-1418-4
8. L.M. Rossi, A.D. Quach and Z. Rosenzweig, *Anal. Bioanal. Chem.*, 380 (2004) 606-613
9. J.P. Li, X.P. Wei and Y.H. Yong, *Sens. Actuat. B: Chem.*, 139 (2009) 400-406
10. A.Doron, E. Katz and I. Willner, *Langmuir*, 11 (1995) 1313-1317
11. X. Cao, Y. Ye and S. Liu, *Anal. Biochem.*, 417 (2011) 1-16
12. C. X. Lei, S.Q. Hua, G..L. Shen and R.Q. Yu, *Talanta*, 59 (2003) 981-988
13. J. Li, L.T. Xiao, X.M. Liu, G..M. Zeng, G.H. Huang, G.L. Shen and R.Q. Yu, *Anal. Bioanal. Chem.*, 376 (2003) 902-907
14. H. Yin, S. Ai, W. Shi and L. Zhu, *Sens. Actuat. B: Chem.*, 137 (2009) 747-753
15. J.P. Li, H.L. Gao, Z.Q. Chen, X.P. Wei and C.F. Yang, *Anal. Chim. Acta*, 655 (2010) 98-104
16. M.S. Lin and H.J. Leu, *Electroanalysis*, 17 (2005) 2068-2073
17. F. Wang, R. Yuan, Y. Chai and D. Tang, *Anal. Bioanal. Chem*., 387 (2007) 709-717
18. J. Zhuang, J. Zhang, L. Gao, Y. Zhang, N. Gu, J. Feng, D. Yang and X. Yan, *Mat. Lett.*, 62 (2008) 3972-3974
19. G.S. Lai, H.L. Zhang and D.Y. Han, *Sens. Actuat. B: Chem*., 129 (2008) 497-503
20. H.L. Zhang , G.S. Lai, D.Y. Han and A.M. Yu, *Anal. Bioanal. Chem*., 390 (2008) 971-977
21. Q. Chang, K. Deng, L. Zhu , G. Jiang, C. Yu and H. Tang, *Microchim. Acta*, 165 (2009) 299-305
22. X. Tan, J. Zhang, S. Tan, D. Zhao, Z. Huang, Y. Mi and Z. Huang, *Electroanalysis*, 21 (2009) 1514-1520
23. X. Chen, T. Zhao and J. Zou, *Microchim. Acta*, 164 (2009) 93-99
24. S. Chen, R. Yuan, Y. Chai, B. Yin, W. Li and L. Min, *Electrochim. Acta*, 54 (2009) 3039-3046
25. J.P. Li and H.L. Gao, *Electroanalysis*, 20 (2008) 881-887
26. G. Frens, *Nature (Phys. Sci.)*, 241 (1973) 20-22
27. S. Sun and H. Zeng, *J. Am. Chem. Soc.*, 124 (2002) 8204-8205
28. Y.C. Chang and D.H. Chen, *J. Colloid Interf. Sci*., 283 (2005) 446-451
29. W.M. Deen and B. Satvat, *Am. J. Physiol*. *Renal. Physiol*., 241 (1981) F162-F170
30. P. George. *Nature*, 169 (1952) 612-613
31. Y. Xiao, H.X. Ju and H.Y. Chen, *Anal. Biochem.*, 278 (2000) 22-28
32. C. Ruan, F. Yang, C. Lei and J. Deng, *Anal. Chem*., 70 (1998) 1721-1725
33. C. Ren, Y. Song, Z. Li and G. Zhu, *Anal. Bioanal. Chem*., 381 (2005) 1179-1185
34. Z. Tong, R. Yuan, Y. Chai, Y. Xie, *J.* Biotechnol. 2007,*128*, 567-575
35. J. Li, J. Yan, Q. Deng, G. Cheng and S. Dong, *Electrochim. Acta*, 42 (1997) 961-967

© 2011 by ESG (www.electrochemsci.org)